

# A 1024-channel 6 mW/mm<sup>2</sup> Optical Stimulator for In-Vitro Neuroscience Experiments

Lei Cai<sup>1</sup>, Baitong Wang<sup>1</sup>, Xiuxiang Huang<sup>1</sup> and Zhi Yang<sup>1,2</sup>

**Abstract**—Recent optical stimulation technologies allow improved selectivity and have been widely used in neuroscience research. This paper presents an optical stimulator based on high power LEDs. It has 1024 channels and can produce flexible stimulation patterns in each frame, refreshed at above 20 Hz. To increase the light intensity, each LED has an optical package that directs the light into a small angle. To ensure the light of each LED can reach the lens, the LEDs have been specially placed and oriented to the lens. With these efforts, the achieved power efficiency (defined as the amount of LED light power passing through the lens divided by the LED total power consumption) is  $5 \times 10^{-5}$ . In our current prototype, an individual LED unit can source 60mW electrical power, where the induced irradiance on neural tissues is 6 mW/mm<sup>2</sup> integrating from 460nm to 480nm. The light spot is tunable in size from 18  $\mu\text{m}$  to 40  $\mu\text{m}$  with an extra 5-10  $\mu\text{m}$  separation for isolating two adjacent spots. Through both bench-top measurement and finite element simulation, we found the cross channel interference is below 10%. A customized software interface has been developed to control and program the stimulator operation.

## I. INTRODUCTION

Micro electrode arrays (MEAs) have been used in various neuroscience experiments for recording and stimulating neurons since the early 70s [1]. Though a critical technology in both clinical and scientific use, electrical stimulation with MEA has a number of drawbacks. First, electrical stimulation tends to activate a cluster of neurons rather than individual ones. Second, electrical stimulation brings in artifacts that can easily mask the direct neuronal responses and cause amplifier saturation. Third, electrical pulses tend to be excitatory only to the direct neuronal targets. Finally, frequent stimulation can cause damage to both the electrode and tissues.

Optogenetics involves the combination of optic and genetic techniques for the study of neural circuits [2], [3]. Compared with electrical stimulation, optogenetics allows targeting specific types of neurons, simultaneous stimulation and recording [4], and both excitatory and inhibitory modulations [5]. Due to its obvious advantages, the neuroscience community has quickly adopted the technology and since then an explosion of so-called optogenetics research has occurred.

Optical stimulator can be technically challenging to design. Channelrhodopsin-2 (ChR2), the light-sensitive ion-channels of neurons, has an action-spectrum peak at around

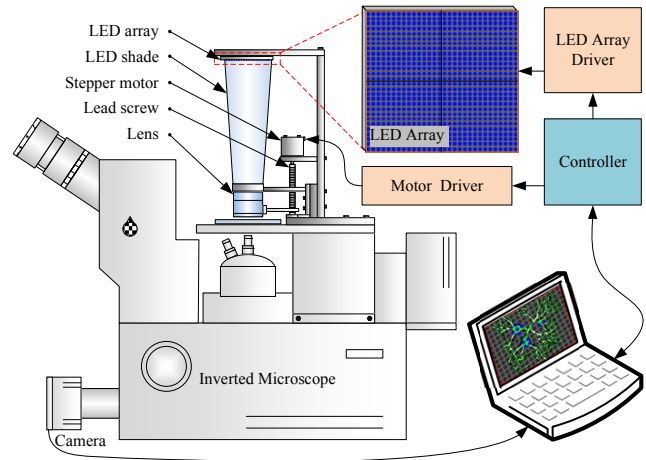


Fig. 1. Illustration of the proposed optical stimulator with 1024 channels. The light produced by the LED array is collected by a lens and projected onto neural tissues.

470 nm [6]. The required spiking irradiance with 470 nm light is between 0.1 and 1 mW/mm<sup>2</sup> [7], which is quite high and has hindered the development of methods for two-dimensional spatiotemporal control. This level of irradiance can be achieved with high power light sources, e.g. arc lamps [4], lasers [8], or high power light-emitting diodes [9,10]. The light sources can be coupled with optical fibers through which light is delivered to the targeting locations [11,12]. Light sources can also be integrated with a digital micro mirror device, where a micro mirror is used to direct light to different locations. Although the mirror can be switched from one location to another within a few  $\mu\text{s}$ , it requires several ms continuous light exposure to activate the targeting neuron [13,14]. As a result, the mirror system can only address some simple patterns with a slow refreshing rate.

Figure 1 illustrates the proposed optical stimulator. The top layer is an LED array driven by a customized circuit board. The board is connected to a computer, where we have developed software that allows users to conveniently program spatial and temporal patterns. The illumination patterns are flexible and can be refreshed at a frame rate above 20 Hz, where each LED can be turned on up to 6ms within one frame. In Figure 2, stimulation pattern examples are displayed, where it takes less than 50ms to switch from one frame to another. Each selected pixel in a frame is on for at least 6ms.

In this paper, we present an optical stimulator that over-

<sup>1</sup>Department of Electrical and Computer Engineering, National University of Singapore

<sup>2</sup>Interactive & Digital Media Institute, National University of Singapore, eleyangz@nus.edu.sg

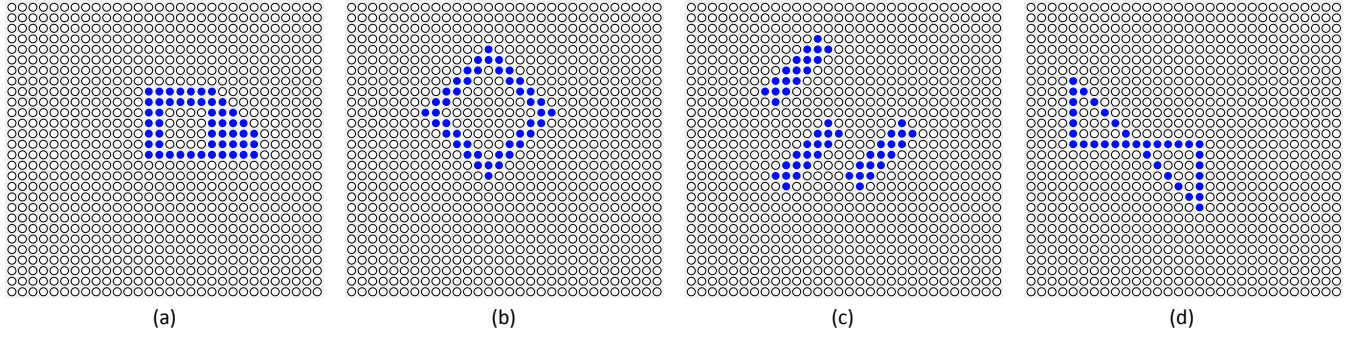


Fig. 2. LED stimulation pattern Examples. It takes less than 50ms to switch one entire frame to another. Each selected channel within one frame is on for at least 6ms.

comes some of the limitations in the current systems. The proposed stimulator has 1024 channels and can produce a flexible stimulation pattern with a refresh rate above 20 Hz. The light spot can be adjusted in size from 18  $\mu\text{m}$  to 40  $\mu\text{m}$  with an extra 5-10  $\mu\text{m}$  separation for isolating two adjacent spots. It also allows targeting neurons at an adjustable depth up to 300  $\mu\text{m}$ . To achieve a high channel count and sufficient irradiance to modulate neurons, we have tried optical package, LED placement, and driver circuits. As a result, the prototype can achieve 6  $\text{mW}/\text{mm}^2$  irradiance on neural tissues at the wave length around 470 nm. There for we have much range of choice and have more light absorb allowance.

The rest of the paper is organized as follows. Section II describes the optical stimulator hardware design. Section III reports the measurement results. Section IV concludes this work.

## II. HARDWARE DESIGN AND ANALYSIS

The power consumption of each LED is adjustable up to 60 mW through software. The light produced by the LED array is collected by a lens and projected onto neural tissues. The distance between the LED array and the lens is tunable and its default value is 20 cm. Due to light spread (as distance increase, light spreads out), only a small portion of the light produced by an LED can reach the lens as shown in Figure 3. For example, assume an LED produces a uniform light distribution within a space angle ( $2\Omega$ ), the portion of light that can reach the lens is roughly

$$p_1 = \begin{cases} l^2 \cos^2 \alpha / 16d^2 \sin^2 \Omega & \text{if } |\alpha| < \Omega, \\ 0 & \text{otherwise,} \end{cases} \quad (1)$$

where  $l$  is the len diameter,  $d$  is LED distance to lens,  $\alpha$  is the angle between the light direction and the lens axis.

To achieve a high imaging precision, only a small area of the lens is transparent to light, which depends on the light orientation. For example, when light orientation is along the lens axis, the percentage of light that can pass through the lens over the light hits the lens surface is

$$p_1 = kW_n^2 / l^2, \quad (2)$$

where  $k$  quantifies the percentage of power loss due to penetration through the lens, around 80%-90% in a measurement;

$W_n$  is the diameter of the transparent area on the lens, around 1mm.

The power efficiency defined as the amount of LED light power passing through the lens divided by the LED total power:

$$p = cp_1 p_2 f_{46-48} = ckf_{46-48} W_n^2 \cos^2 \alpha / 16d^2 \sin^2 \Omega, \quad (3)$$

where  $c$  is the conversion ratio of electrical power to optical power around 25% and  $f_{46-48}$  the optical power integrated from 460nm to 480nm divided by the full bandwidth optical power.

Assume  $c=25\%$ ,  $k=0.8$ ,  $W_n=1\text{mm}$ ,  $\alpha=0$ ,  $d=20\text{cm}$ ,  $\Omega=\pi/4$ , and  $f_{46-48}=0.5$ , the power efficiency is  $0.8 \times 10^{-6}$ : with a 60mW LED, only 48nW optical power within 460-480 nm can penetrate through the lens.

To reduce the power attenuation through spread, each LED has integrated with optical package to direct/focus the light. Figure 4 gives measured optical power intensity with (brown plot) and without (light blue plot) optical package. This allows one order increasing the energy efficiency from  $0.8 \times 10^{-6}$  to  $5 \times 10^{-5}$ . A drawback is that an optical package reduces the  $\Omega$  and achievable channel count, as illustrated in Equation 1 and Figure 5 (a) - (d). In the rest of this section, analysis and design efforts on the proposed stimulator are presented.

### A. Light Path Analysis

As shown in Figure 3, for a circular shaped LED (diameter  $D_l$ ) and a lens (focal length  $f$ ), the diameter of the induced light spot  $D_s$  is

$$D_s = D_l \frac{f}{d-f}, \quad (4)$$

where  $d$  is the distance between the LED and the lens.

Assuming the lens has light transmittance  $\eta$  and the input optical power is  $W_n$ , the averaged irradiance within the stimulation spot  $I_s$  is approximately

$$I_s = \frac{W_s}{S_s} = \frac{4W_n \eta}{\pi} \left( \frac{d-f}{D_l f} \right)^2, \quad (5)$$

where  $W_s$  is the output power from the lens and  $S_s$  is the area of the stimulation spot.

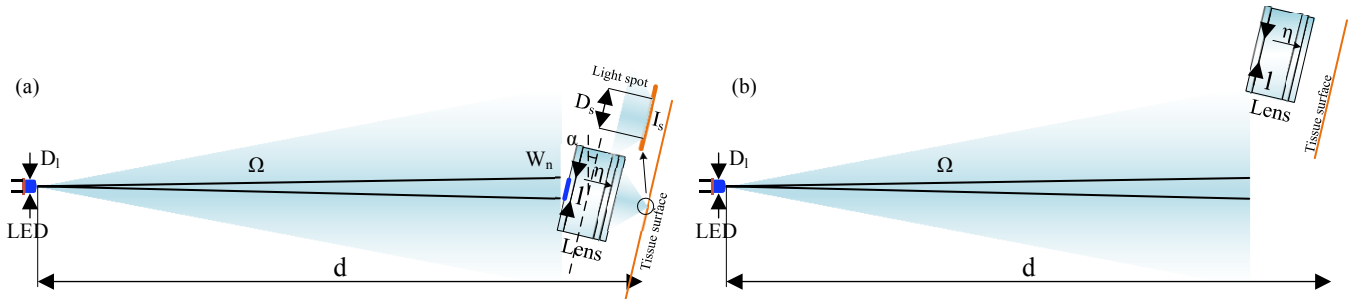


Fig. 3. Illustration of the light path from one single LED. Only light in a very small  $W_n$  can penetrate through the lens.

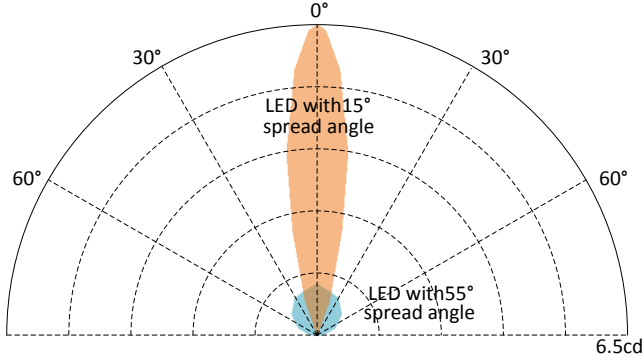


Fig. 4. Measured LED radiation patterns. Brown plot and light blue plot are measurement with and without optical package.

The luminosity function  $V(\lambda)$  converts photometric into radiometric measurements is

$$I_v = 683 \int_0^\infty V(\lambda) k \bar{I}_e(\lambda) d\lambda, \quad (6)$$

where  $I_v$  is luminous intensity in candelas ( $cd$ ),  $V(\lambda)$  is the standard luminosity function,  $\bar{I}_e(\lambda)$  is relative radiant intensity distribution in watts per steradian and meter ( $W/(m \cdot sr)$ ) and  $k$  is a coefficient of  $\bar{I}_e(\lambda)$ .

With  $I_v$ ,  $V(\lambda)$ , and  $\bar{I}_e$  obtained, the induced irradiance inside the stimulation spot  $I_s$  is

$$I_s = \frac{8\eta I_v \int_0^\infty \bar{I}_e(\lambda) d\lambda}{683 \int_0^\infty V(\lambda) \bar{I}_e(\lambda) d\lambda} \left(1 - \frac{2D_l f_\#}{\sqrt{4D_l^2 f_\#^2 + f^2}}\right) \left(\frac{d-f}{D_l f}\right)^2. \quad (7)$$

where  $f_\#$  is  $f$  number of the lens.

### B. Orientation of LED Arrays

A high channel count LED array is constrained by the spread angle and the required irradiance intensity at the lens, as illustrated in Fig. 5(a)-(d). On the one hand, LEDs with a large spread angle can reach the lens, at the cost of compromised irradiance intensity. On the other hand, LEDs with a small spread angle can have high irradiance along the normal direction. However, the achievable channel count is low.

To resolve the trade off between the channel count and irradiance strength, we propose a special layout for the LED array. As shown in Fig. 5(e), the orientation of each LED

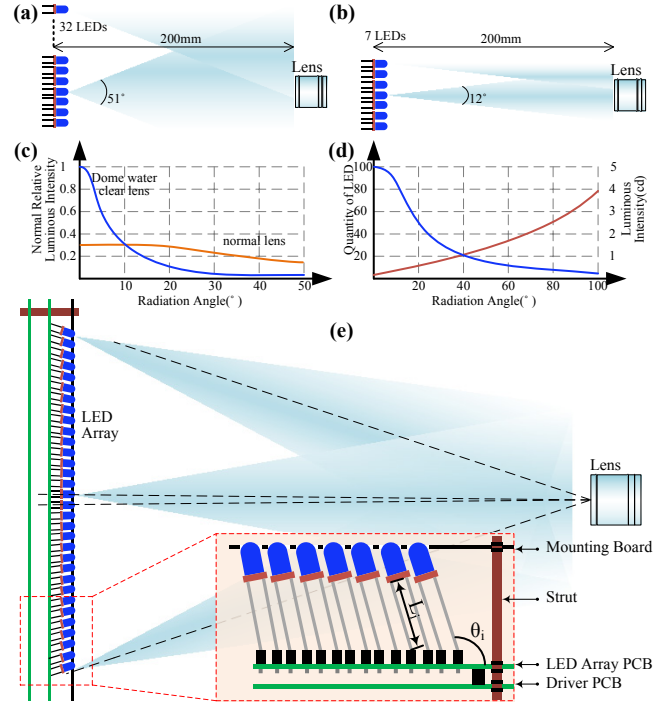


Fig. 5. The trade off between the channel count and the irradiance intensity. (a) illustrates LEDs with wide spread angle but low irradiance. (b) illustrates LEDs with small spread angle but high irradiance intensity. (c) sketches the relationship between the spread angle (x axis) and irradiance intensity (y axis). (d) shows the LED count vs the spread angle. (e) shows the principal of LED array package.

is specifically adjusted such that all LEDs head towards the lens

$$x_{ij} = 5.08i - 2.54 + 1.27 \cos \theta_{ij} + \frac{200 \sqrt{(5.08i - 2.54)^2 + (5.08j - 2.54)^2}}{\sqrt{1 + \tan^2 \theta_{ij}}} \quad (8)$$

$$y_{ij} = 5.08j - 2.54 + 1.27 \cos \theta_{ij} + \frac{200 \sqrt{(5.08j - 2.54)^2 + (5.08i - 2.54)^2}}{\sqrt{1 + \tan^2 \theta_{ij}}} \quad (9)$$

$$\theta_{ij} = \arctan \sqrt{(4i - 2)^2 + (4j - 2)^2}, i, j = 1, 2, 3 \dots 16 \quad (10)$$

Equations (8)-(10) give the theoretical values of X, Y, and orientation ( $x_{ij}$ ,  $y_{ij}$ , and  $\theta_{ij}$ ) for achieving the highest

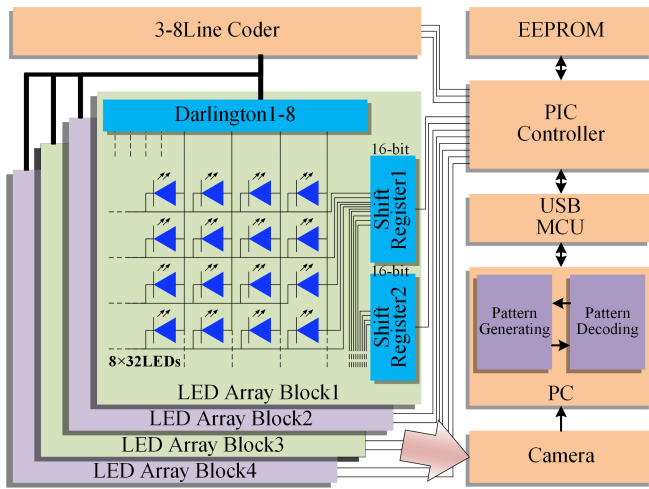


Fig. 6. Illustration of the stimulator drivers and controller.

irradiance. In the current prototype, we have placed LEDs close to their ideal locations, where we can maximally increase the LED count up to 10,000 channels since the view angle of the lens in use is  $80^\circ$  and the diameter of each LED is in mm size.

### C. LED Driver, Controller, and Interface

The stimulation pattern can be programmed on the PC and downloaded to the proposed system through a USB-SPI IC (PIC18f4550). A micro-controller (PIC32MX340F128L) is used to coordinate system operation. As showed in Figure 6, to balance the processing delay and the programming selectivity of individual LEDs, the  $32 \times 32$  array is divided into four blocks ( $8 \times 32$ ), each of which is addressed by applying a positive bias voltage across its row and a zero voltage across its column.

Every 16 LEDs are driven by a current sink (STP16DP05) with an embedded shift register, which can provide 20 mA constant current to drive the LEDs. To turn on the same rows (each row has 32 LEDs) in 4 blocks at the same time, 2.56 A current are required and coordinated by darlington transistors (TIP127). Both the transistors and the current sinks are controlled by the micro-controller. When the device is active, the micro-controller keeps scanning a buffer to update user-defined patterns, and outputs command bits to change the driving current and the pulse width duty cycle of each LED.

## III. RESULTS

Figure 8(a) shows the proposed stimulator prototype, where the LEDs are controlled by the customized software/hardware interface. The diameter of each light spot is  $24 \mu\text{m}$ , measured by a high precision imager. A snapshot of measurement is shown in Fig. 8(b).

The LED has a luminous intensity of 8.2 cd when the driving current is 32 mA and 17 cd at 80 mA, as shown in Fig. 7(a). We found out high LED current reduces the prototype life time. As a result, we only use up to 20mA in experiments. In Fig. 7(b), the emission spectrum of each

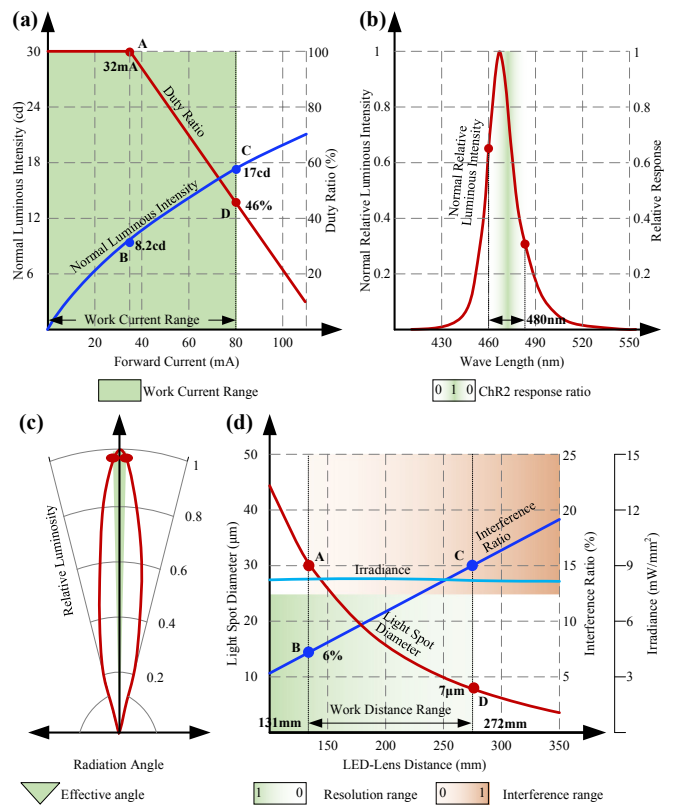


Fig. 7. (a) LED luminous intensity vs. current duty cycle, (b) LED power spectrum, (c) shows the radiant angle of an LED, (d) shows the allowable distance between the LED array and the lens 131mm-272mm.

LED is centred at 470 nm with only 20 nm full width half maximum, overlapping with the peak sensitivity range of ChR2. In our system, there is measured 4mW optical power within 6 degree spread angle when the LED is powered at 20mA. Fig. 7(d) shows that the increasing of the LED-lens distance will decrease the diameter of light spots and aggravate the interference between channels. Meanwhile, the irradiance intensity is almost the same due to the simultaneously decreasing of light spots area. According to these variations, the optimal work distance range is from 131 mm to 272 mm.

The focal length of the lens (LMVZ256) ranges from 2.5 mm to 6 mm and the  $f$  number of the lens ranges from 1.4 to  $+\infty$ . The distance from LED to lens is by default set at 200 mm. The irradiance is measured by an optical power meter (ADCMT8230 with 82311B sensor). Fig. 9 illustrates the measured irradiance of sampled spots, which is above  $6 \text{ mW/mm}^2$  with a  $5 \mu\text{m}$  interference between two adjacent light spots.

By moving the LED array/lens along the Z direction, the proposed system has a Z selectivity at a depth up to 300  $\mu\text{m}$ . Fig. 10(a) illustrates the simulated irradiance (by TRACEPRO) in the XZ plane with liquid and neural tissues added into the simulation environment. Fig. 10(b) gives the contour map of the irradiance.





Fig. 8. (a) Stimulator prototype. The LED array is controlled by a PC interface through a micro controller. There is a high precision imager recording the stimulation patterns. The measurement results are display on the same PC in real time. (b) snapshot of measured stimulation pixels.

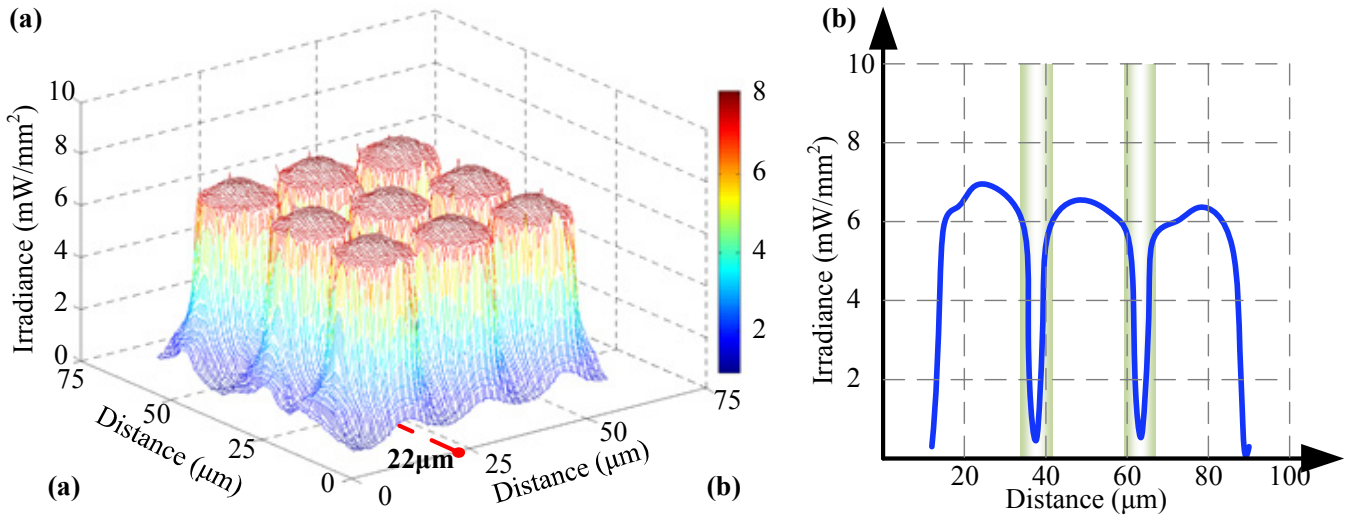


Fig. 9. (a) Measured irradiance distribution in XY plane. (b) Measured irradiance along one dimension to sketch possible cross-channel interference.

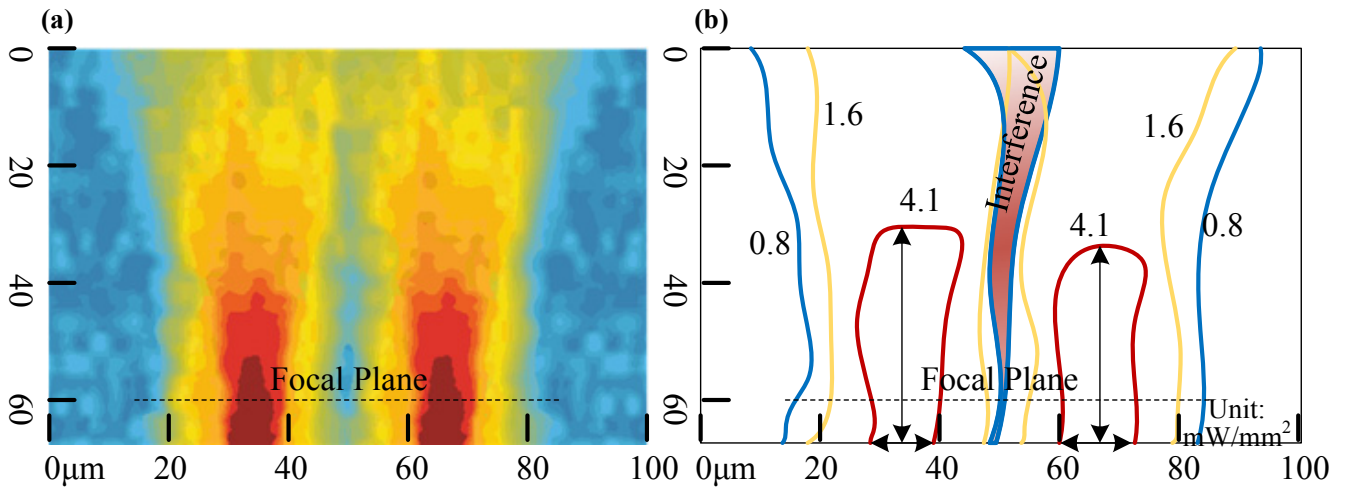


Fig. 10. (a) Simulated irradiance (by TRACEPRO) in XZ plane with focal place set at  $z=60\mu\text{m}$ . Liquid and neural tissues have been added into the simulation model. (b) Contour map of the irradiance in (a).

#### IV. CONCLUSION

This paper presents an optical stimulator based on high power LEDs. It has 1024 channels and can produce flexible

stimulation patterns in each frame at a refreshing rate of 20 Hz. The light spot is tunable in size from  $18\ \mu\text{m}$  to

40  $\mu\text{m}$  with an extra 5-10  $\mu\text{m}$  separation for isolating two adjacent spots. Different from many other designs, the proposed stimulator allows Z selectivity at a depth varied from 0 to 300  $\mu\text{m}$ . To achieve a high channel count and sufficient irradiance to modulate neurons, we have proposed several novel engineering techniques, achieving 6  $\text{mW}/\text{mm}^2$  irradiance near the wavelength of 470 nm.

#### V. ACKNOWLEDGEMENT

This research is supported by Singapore Young Investigator Grant R-263-000-A29-133.

#### REFERENCES

- [1] Charles Thomas, et al, "A miniature microelectrode array to monitor the bioelectric activity of cultured cells," *Experimental cell research*, 74.1 (1972): 61-66.
- [2] Edward Boyden, et al, "Millisecond-timescale, genetically targeted optical control of neural activity," *Nature neuroscience* 8.9 (2005): 1263-1268.
- [3] Feng Zhang, et al, "Channelrhodopsin-2 and optical control of excitable cells," *Nature methods* 3.10 (2006): 785-792.
- [4] O Yizhar, et al, "Optogenetics in neural systems," *Neuron* 71.1 (2011): 9-34.
- [5] Karl Deisseroth, "Optogenetics," *Nature methods* 8.1 (2010): 26-29.
- [6] Klapoetke, et al. "Independent optical excitation of distinct neural populations." *Nature Methods* 11.3 (2014): 338-346.
- [7] Nir Grossman, et al, "Multi-site optical excitation using ChR2 and micro-LED array," *Journal of neural engineering* 7.1 (2010): 016004.
- [8] Werner Gobel, et al, "Imaging cellular network dynamics in three dimensions using fast 3D laser scanning," *Nature Methods* 4.1 (2006): 73-79.
- [9] Steven Sun, et al, "Multi-wavelength Spatial LED illumination based detector for in vitro detection of Botulinum Neurotoxin A Activity," *Sensors and Actuators B: Chemical* 146.1 (2010): 297-306.
- [10] Seiichiro Sakai, et al, "Parallel and patterned optogenetic manipulation of neurons in the brain slice using a DMD-based projector," *Neuroscience Research* (2012).
- [11] Berlinguer Palmieri, et al, "A New Individually Addressable Micro-LED Array for Photogenetic Neural Stimulation," *Biomedical Circuits and Systems*, 4.6 (2010): 469-476.
- [12] Suzurikawa, Jun, et al. "Light-Addressed Stimulation and Simultaneous Calcium Imaging for Probing Spatio-Temporal Activity of Cultured Neural Network." *Neural Engineering*, 2007: 269-276.
- [13] Poher, V., et al. "Micro-LED arrays: a tool for two-dimensional neuron stimulation." *Journal of Physics D: Applied Physics* 41.9 (2008): 094014.
- [14] Atallah Bassam V., et al. "Parvalbumin-expressing interneurons linearly transform cortical responses to visual stimuli." *Neuron* 73.1 (2012): 159-170.